

Shock waves in Stokes flows down an inclined plate

E. S. Benilov* and V. N. Lapin†

Department of Mathematics, University of Limerick, Ireland

(Received 13 December 2010; published 29 June 2011)

We consider a viscous flow on an inclined plate, such that the liquid's depth far upstream is larger than that far downstream, resulting in a "smoothed-shock wave" steadily propagating downstream. Our numerical simulations show that in a large section of the problem's parameter space all initial conditions overturn (i.e., the liquid's surface becomes vertical at some point) and thus no steady solution exists. The overturning can only be stopped by a sufficiently strong surface tension.

 DOI: [10.1103/PhysRevE.83.066321](https://doi.org/10.1103/PhysRevE.83.066321)

PACS number(s): 47.55.N-, 47.35.Jk

I. INTRODUCTION

Consider a layer of viscous liquid on a sloping plate (see Fig. 1), and let the layer's depth far upstream be larger than that far downstream. In this case, one could expect a "smooth-shock wave" (SSW) to steadily propagate down the plate.

So far this classical problem has been mostly examined for *thin* flows, for which the slope of the free surface is small. In this case, the long-wave approximation can be employed using which Benney [1] reduced the Navier–Stokes set to a single asymptotic equation and showed that, under an extra assumption of weak nonlinearity, it can be reduced further to either the Korteweg–de Vries equation or the Burgers equation. Employing the long-wave approximation under slightly different limits, Mei [2] derived the Burgers–Korteweg–de Vries equation, whereas Homsy [3], Nepomnyashchy [4], and Lin [5] derived the Kuramoto–Sivashinsky equation (see also [6] and references therein). The case of two thin (long-wave) layers with different densities and viscosities was examined by Mavroustaki, Matar, and Craster [7]. Note that, in all of the above models, SSWs exist for all values of the parameters involved.

The present work examines SSWs in a one-layer liquid without the long-wave approximation. Our main conclusion is that, in a significant part of the parameter space, steady SSWs do not exist due to overturning.

II. FORMULATION

Consider a layer of liquid on a rigid plate inclined at an angle α (see Fig. 1). Denote the acceleration due to gravity by g and the layer's depths far upstream and far downstream by $H^{(+)}$ and $H^{(-)}$, respectively.

Let the liquid's density, viscosity, and surface tension be ρ , μ , and σ . Then, as demonstrated below, the velocity of an SSW, if it exists, is

$$U = \frac{(H^{(+2)} + H^{(+)}H^{(-)} + H^{(-2)})\rho g \sin \alpha}{3\mu}. \quad (1)$$

To nondimensionalize the problem we use U as the velocity scale and $H = (vU/g \sin \alpha)^{1/2}$ as the scale for the spatial coordinates and the liquid's depth. H/U and $\rho H g \sin \alpha$ are used as the time and pressure scales.

The flow will be modeled using the nondimensional Stokes equations

$$p_x = -1 + u_{xx} + u_{yy}, \quad p_y = -\cot \alpha + v_{xx} + v_{yy}, \quad (2)$$

$$u_x + v_y = 0, \quad (3)$$

where the x axis (y axis) is directed along (perpendicular to) the plate, u and v are the x and y components of the liquid's velocity, t is the time, and p is the pressure. Instead of assuming that the SSW is steadily propagating down the plate, we let the plate move up with the matching velocity, so the boundary conditions at the plate-liquid interface are

$$u = 1, \quad v = 0 \quad \text{at } y = 0. \quad (4)$$

We shall use the standard set of boundary conditions at the liquid's free surface,

$$\left. \begin{aligned} h_t + u h_x - v &= 0, \\ \mathbf{n}^T \mathbf{S} \mathbf{n} &= \gamma C, \quad \tau^T \mathbf{S} \mathbf{n} = 0 \end{aligned} \right\} \quad \text{at } y = h, \quad (5)$$

where h is the nondimensional depth, $\gamma = \sigma/\mu U$ is the capillary coefficient, the superscript T denotes matrix transposition, and

$$\mathbf{n} = \frac{1}{[1 + (h_x)^2]^{1/2}} \begin{bmatrix} -1 \\ h_x \end{bmatrix}, \quad \tau = \begin{bmatrix} h_x \\ 1 \end{bmatrix} \quad (6)$$

are the unit normal vector and a tangent vector (not necessarily unit) to the free surface; and

$$\mathbf{S} = \begin{bmatrix} 2u_x - p & u_y + v_x \\ u_y + v_x & 2v_y - p \end{bmatrix}, \quad C = \frac{h_{xx}}{[1 + (h_x)^2]^{3/2}} \quad (7)$$

are the stress tensor and the curvature of the free surface. Finally, we assume

$$h \rightarrow h^{(\pm)} \quad \text{as } x \rightarrow \pm\infty, \quad (8)$$

where $h^{(\pm)}$ are the nondimensional counterparts of $H^{(\pm)}$ (see Fig. 1).

It can be demonstrated that steady solutions of Eqs. (2)–(7) satisfy

$$\int_0^h u \, dy = q, \quad (9)$$

*Eugene.Benilov@ul.ie

†Vladimir.Lapin@ul.ie

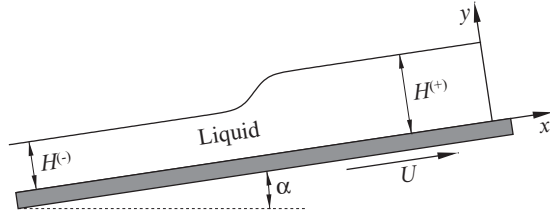


FIG. 1. The setting: a smooth-shock wave (SSW) on an inclined plate.

where the constant of integration q is, physically, the nondimensional liquid flux along the plate. It can also be shown that the boundary conditions (8), together with Eqs. (2)–(7), imply

$$\left. \begin{aligned} u &\rightarrow 1 - yh^{(\pm)} + \frac{1}{2}y^2, \\ v &\rightarrow 0, \\ p &\rightarrow (h^{(\pm)} - y) \cot \alpha \end{aligned} \right\} \text{ as } x \rightarrow \pm\infty. \quad (10)$$

Substitution of (10) into (9) yields

$$h^{(\pm)} - \frac{1}{3}h^{(\pm)3} = q. \quad (11)$$

Recalling how our variables were nondimensionalized, one can use (11) to obtain (1) and also an expression for the nondimensional flux,

$$q = \frac{3^{1/2} H^{(+)} H^{(-)} (H^{(+)} + H^{(-)})}{(H^{(+2)} + H^{(+)} H^{(-)} + H^{(-2)})^{3/2}}.$$

Thus, our problem [governed by Eqs. (2)–(8), and (11)] is fully determined by three nondimensional parameters: q , γ , and α . Note that (11) implies that

$$0 < q < \frac{2}{3}, \quad 0 < h^{(-)} < 1, \quad 1 < h^{(+)} < 3^{1/2}, \quad (12)$$

with $q = 0$ corresponding to $h^{(-)} = 0$, $h^{(+)} = 3^{1/2}$.

III. THE NUMERICAL METHOD

Equations (2)–(8), and (11) were integrated numerically, using the finite-element solver of the COMSOL [8] Multiphysics package. We used the module for two-dimensional incompressible Navier–Stokes equations. The physical parameters were chosen in such a way that the Reynolds number Re was very small ($Re = 10^{-4}$), so the results obtained would provide an accurate approximation of the Stokes equations (2) and (3). The boundary conditions as $x \rightarrow \pm\infty$ were modeled by sources located far upstream and sinks located far downstream, both distributed along the vertical intervals $0 < y < h^{(\pm)}$. The intensities of the sources and sinks and the boundary pressure profiles depended on y in accordance with (10). The computations were carried out using the *moving mesh* mode incorporating the *arbitrary Lagrangian-Eulerian* (ALE) method, which allows the mesh to track the moving boundary. At the free boundary, the normal component of the mesh velocity was equal to the normal component of the liquid’s velocity, and at the fixed boundaries the mesh was constrained to have zero normal displacement. Within the domain, the nodes’ motion was unconstrained and computed by the software to optimize the elements’ quality. Typically, the discretized problem contained about 50 000 degrees of freedom and was solved through either the PARDISO [9] or the UMFPAK [10] solver.

For the initial condition, we mostly used the steady-state solution for a case with similar parameter values. If such was not available, a smoothed step function was used for h , the hydrostatic pressure distribution for p , and the expressions predicted by the lubrication approximation for u and v . Even though such conditions did not exactly satisfy the Stokes equations, they were automatically adjusted by the software and a self-consistent initial flow was generated. Then, Eqs. (2)–(8) were integrated until a steady state was established.

Test simulations with decreasing mesh sizes and relative or absolute tolerances, and different initial conditions were performed to insure that the results converged to the same solutions and, thus, were robust.

Note that solutions with $\alpha \approx 0^\circ$ or $\alpha \approx 90^\circ$ are difficult to compute. In the former case, $h^{(-)}$ is very small, which necessitates extreme refinement of the mesh. In the latter case, the SSWs have oscillatory structure spreading over a large region (for more details, see below), which necessitates extreme enlargement of the computational domain. Therefore, the results for $\alpha = 90^\circ$ were extrapolated using those for neighboring values of α , whereas the result for $\alpha = 0^\circ$ can be deduced analytically using the lubrication approximation.

IV. THE RESULTS

A. The case $\gamma = 0$

For zero surface tension, a unique SSW solution was found in a certain region of the (α, q) plane [see Fig. 2(a)]. Examples of SSWs are shown in Fig. 3: one can see that the solution for $\alpha = 70^\circ$ has an oscillatory structure. Those for $\alpha = 50^\circ$ and $\alpha = 30^\circ$ also oscillate, but the oscillations decay so rapidly that they are not visible in Fig. 3 (but are readily detectable in the numeric data). This comes as a surprise, as the problem involves neither capillary nor gravity waves (the former have been eliminated by the assumption $\gamma = 0$ and the latter by using the Stokes equations neglecting the liquid’s inertia). This issue will be discussed in detail later, whereas here we just note that oscillating SSWs have been previously observed in Ref. [2] (where, unlike this work, the liquid’s inertia was indeed taken into account).

Another surprising result is that, for any value of the flux q , there is a critical angle $\alpha_{cr}(q)$ such that for $\alpha > \alpha_{cr}$ all initial conditions overturn, that is, h_x becomes infinite at some x and t (see an example in Fig. 4). We conclude that in a certain region of the problem’s parameter space steady SSWs do not exist.

One might wonder, however, if some of the initial conditions that were *not* simulated would evolve toward a steady SSW. To eliminate this possibility, we employed an approach used in Ref. [11] for a similar problem—namely sufficiently strong surface tension was introduced to the problem, which would stop the overturning and give rise to a steady SSW. Then surface tension was gradually phased out and, if overturning still occurred, we could reliably conclude that no steady solution exists for these values of q and α .

Finally, even though we could not compute $\alpha_{cr}(q)$ for small α , we assumed $\alpha_{cr}(0) = 0$ [see Fig. 2(a)]. To understand why, observe that in the limit $\alpha \rightarrow 0$ one can use the lubrication approximation which yields a steady smooth SSW for any $q > 0$ and a “marginally overturned” SSW (i.e., one with an infinite h_x at a single point) for $q = 0$.

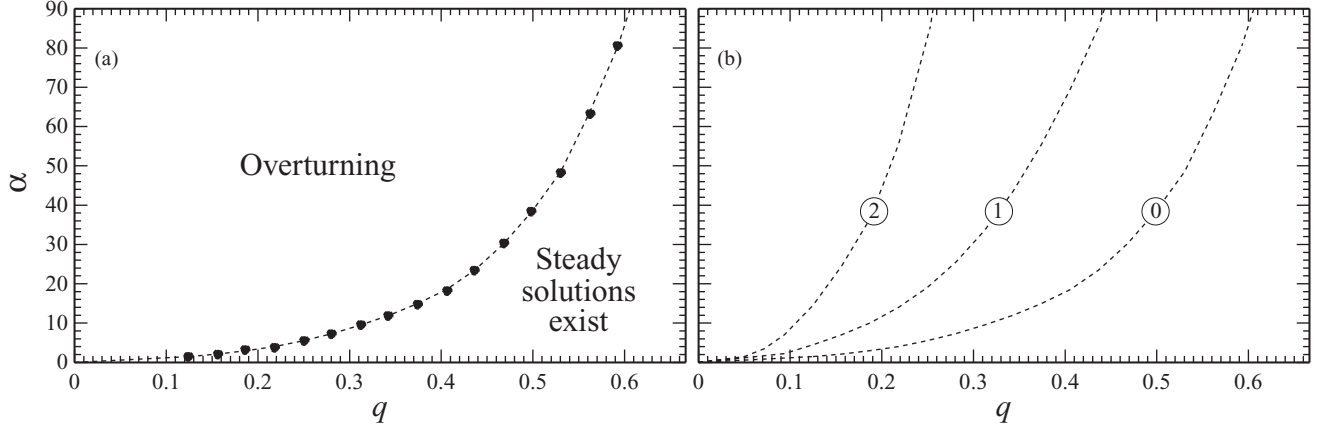


FIG. 2. Existence of SSWs on the (q, α) plane (α is the plate's inclination angle, q is the nondimensional liquid flux). (a) The limit of zero surface tension ($\gamma = 0$). A black dot at a position $\alpha = \alpha_0$ indicates that solutions exist for $\alpha < \alpha_0 - 0.5^\circ$, and solutions do not exist for $\alpha > \alpha_0 + 0.5^\circ$. (b) Curve 0 is the same as that in (a), that is, for $\gamma = 0$. Curves 1, 2 are for $\gamma = 0.5, 1.0$, respectively.

B. The case $\gamma \neq 0$

As mentioned above, surface tension acts against overturning. Thus, with increasing γ , the region in the parameter space where SSW exist expands [see Fig. 2(b)]; however, the “nonexistence” region appears to never disappear completely. Note that, as before, $\alpha_{cr}(0) = 0$, which follows from the asymptotic solution of the problem as $\alpha, q \rightarrow 0$ (see Ref. [12]). Note also that with increasing γ the solution becomes difficult to compute, so the error interval for curves 1 and 2 in Fig. 3(b) is up to $\pm 1.5^\circ$ (as opposed to curve 1, where it is $\pm 0.5^\circ$).

In the cases where overturning does *not* occur, surface tension has little effect on those solutions that do not oscillate for $\gamma = 0$, whereas the solutions that do oscillate for $\gamma = 0$ are made noticeably smoother by the capillary effects (see examples in Fig. 5).

V. OSCILLATORY STRUCTURE OF SSWs FOR $\gamma = 0$

The nature of the solution's oscillations for $\gamma = 0$ can be clarified by assuming that their amplitude is small (which it

indeed is far from the shock). In this case, the steady solution of Stokes set (2)–(7) can be represented in the form

$$\begin{aligned} u &= \bar{u}(y) + \tilde{u}(x, y), & v &= \tilde{v}(x, y), \\ p &= \bar{p}(y) + \tilde{p}(x, y), & h &= \bar{h} + \tilde{h}(x, y), \end{aligned} \quad (13)$$

where the variables with overbars describe the mean flow and tildes describe the small oscillations. The former can be extracted from (10), that is,

$$\bar{u} = 1 - y\bar{h} + \frac{1}{2}y^2, \quad \bar{p} = (h - y) \cot \alpha, \quad (14)$$

with $\bar{h} = h^{(+)}$ ($\bar{h} = h^{(-)}$) for the regions above (below) the shock. Substituting (13) and (14) into Eqs. (2)–(7) with $\gamma = 0$ and linearizing them, we obtain

$$\tilde{p}_x = \tilde{u}_{xx} + \tilde{u}_{yy}, \quad \tilde{p}_y = \tilde{v}_{xx} + \tilde{v}_{yy}, \quad \tilde{u}_x + \tilde{v}_y = 0, \quad (15)$$

$$\tilde{u} = 0, \quad \tilde{v} = 0 \quad \text{at } y = 0, \quad (16)$$

$$\left. \begin{aligned} \bar{u}\tilde{h}_x - \tilde{v} &= 0, \\ \tilde{u}_y + \bar{u}_{yy}\tilde{h} + \tilde{v}_x + \bar{p}\tilde{h}_x &= 0, \\ 2\tilde{v}_y - \bar{p} - \bar{p}_y\tilde{h} - \bar{u}_y\tilde{h}_x &= 0 \end{aligned} \right\} \quad \text{at } y = \bar{h}. \quad (17)$$

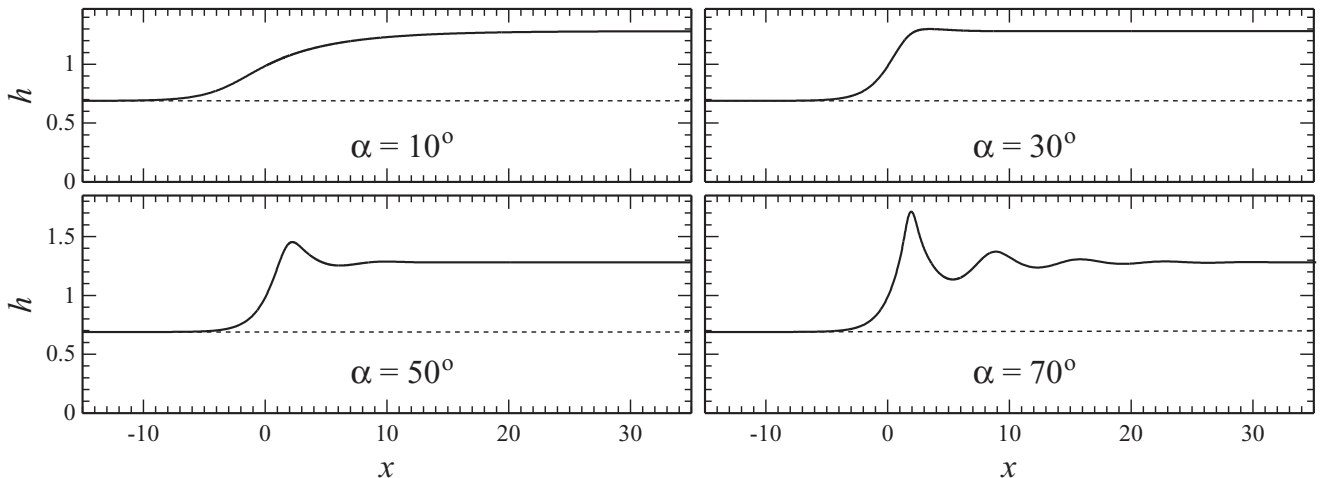


FIG. 3. Examples of SSWs for $\gamma = 0$, $q = 0.58$, and various values of α .

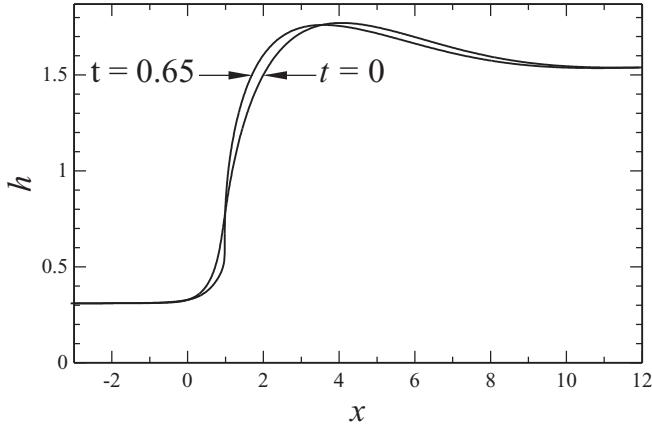


FIG. 4. An example of an overturning SSWs for $\gamma = 0$, $q = 0.3$, $\alpha = 50^\circ$. The “snapshots” are labeled by the corresponding values of the time t .

Equations (14)–(17) admit a solution of the form

$$\begin{aligned} \tilde{u} &= \hat{u}(y)e^{-kx}, & \tilde{v} &= \hat{v}(y)e^{-kx}, \\ \tilde{p} &= \hat{p}(y)e^{-kx}, & \tilde{h} &= \hat{h}e^{-kx}, \end{aligned} \quad (18)$$

where k may be complex, in which case $\text{Re}k$ and $\text{Im}k$ represent the decay rate and wave number of the oscillations, respectively. Substitution of (18) into (14)–(17) yields a boundary-value problem for \hat{u} , \hat{v} , \hat{p} , and \hat{h} ,

$$-k\hat{p} = k^2\hat{u} + \hat{u}_{yy}, \quad \hat{p}_y = k^2\hat{v} + \hat{v}_{yy}, \quad (19)$$

$$-k\hat{u} + \hat{v}_y = 0, \quad (20)$$

$$\hat{u} = 0, \quad \hat{v} = 0 \quad \text{at } y = 0, \quad (21)$$

$$\left. \begin{aligned} -k\left(1 - \frac{1}{2}\hat{h}^2\right)\hat{h} - \hat{v} &= 0, \\ \hat{u}_y + \hat{h} - k\hat{v} &= 0, \\ 2\hat{v}_y - \hat{p} + \hat{h}\cot\alpha &= 0 \end{aligned} \right\} \quad \text{at } y = \bar{h}. \quad (22)$$

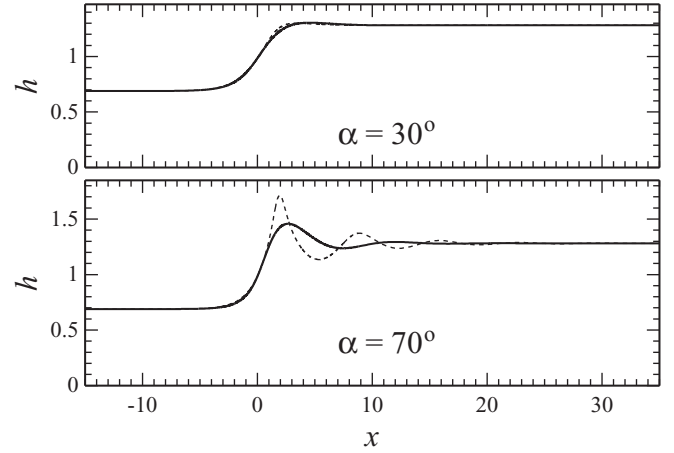


FIG. 5. Examples of SSWs affected by surface tension for $\gamma = 1$, $q = 0.58$, and $\alpha = 30^\circ, 70^\circ$. The dotted line shows the corresponding solutions for $\gamma = 0$ (i.e., the same as in the right-hand panels of Fig. 3).

The general solution of Eqs. (19) and (20) can be readily found,

$$\hat{u} = k^{-1} \{ [k(A_1 + A_2y) + B_2] \cos ky + [A_2 - k(B_1 + B_2y)] \sin ky \}, \quad (23)$$

$$\hat{v} = (A_1 + A_2y) \sin ky + (B_1 + B_2y) \cos ky, \quad (24)$$

$$\hat{p} = 2(A_2 \sin ky + B_2 \cos ky), \quad (25)$$

where $A_{1,2}$ and $B_{1,2}$ are constants of integration. Substituting expressions (23)–(25) into the boundary conditions (21) and (22) and eliminating $A_{1,2}$, $B_{1,2}$, and \hat{h} , we obtain an equation for k ,

$$\frac{2(k\bar{h})^2 - (2k\bar{h} - \sin 2k\bar{h}) \cot \alpha}{4(k\bar{h})^2 [(k\bar{h})^2 - \cos^2 k\bar{h}]} = \frac{1}{2} - \frac{1}{\bar{h}^2}. \quad (26)$$

The dispersion relation (26) was solved numerically (using the secant method) for various values of α and \bar{h} , and it turned out that infinitely many roots exist with positive real parts (negative

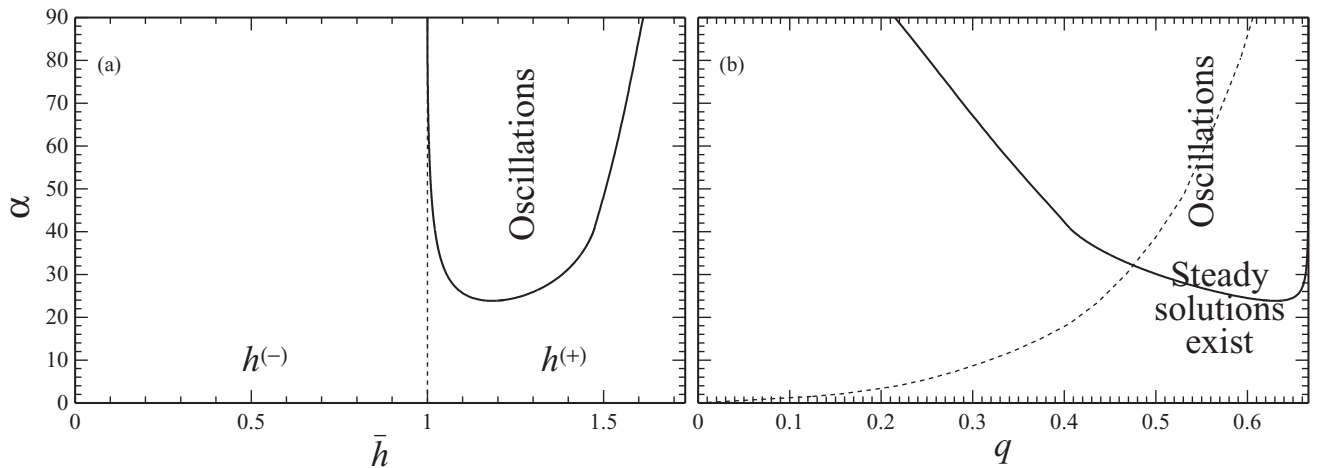


FIG. 6. The parameter range where SSWs have oscillatory structure for $\gamma = 0$: (a) on the (\bar{h}, α) plane; (b) on the (q, α) plane. The ranges for $h^{(\pm)}$ in (a) are determined by (12). The dotted line in (b) shows the region of existence of steady SSWs [i.e., corresponds to curve 0 in Fig. 2(b)].

real parts correspond to meaningless solutions growing as $x \rightarrow +\infty$. We shall denote these roots k_n ($n = 1, 2, 3, \dots$), and order them in such a way that

$$\operatorname{Re} k_{n+1} \geq \operatorname{Re} k_n. \quad (27)$$

Then, the solution of the linearized set (14)–(27) is

$$\tilde{h} = \operatorname{Re} \sum_{n=1}^{\infty} C_n e^{-k_n x}, \quad (28)$$

where C_n are arbitrary complex constants. Given (27), it follows from expression (28) that \tilde{h} , as well as the full solution $\bar{h} + \tilde{h}$, both oscillate as $x \rightarrow +\infty$ if and only if $\operatorname{Im} k_1 \neq 0$.

To find the region in the parameter space where $\operatorname{Im} k_1 \neq 0$, a method was employed which was used previously in Ref. [13]. The results are shown in Fig. 6: clearly a region exists where oscillations are present. Figure 6(a) also shows that all of this region fits into the range for $h^{(+)}$ [determined by (12)], hence oscillations can only be observed *above* (to the right from) the shock. This conclusion agrees with Fig. 3, which indeed shows that the solution below the shock never oscillates.

The values of k_1 computed using Eq. (26) were used to validate our numerical solution of the full nonlinear equations (2)–(8). For $\alpha = 70^\circ$ and $q = 0.58$, for example, (26) yields

$$\pi (\operatorname{Im} k_1)^{-1} \approx 3.475. \quad (29)$$

This value is to be compared with the distances between two successive zeros of the function $h(x) - h^{(+)}$, where $h(x)$ is the steady solution of (2)–(8) computed for the same α and q . According to our simulations, these distances are 2.609, 3.919, 3.249, 3.598, 3.410, 3.511, 3.456, 3.486, 3.470, 3.478, 3.473... (this sequence was truncated near the right-hand boundary of the computational domain, as further measurements would be unreliable). Clearly the measured values rapidly converge onto the “theoretical” value (29).

VI. CONCLUDING REMARKS

It remains to discuss what happens when no steady SSW exists. One can conjecture that in such cases the solution evolves periodically: after overturning, the film’s surface evens out—then a new shock forms and overturns—and so on. This scenario cannot be simulated for the want of a numerical method capable of describing overturning beyond its initial stage, so an experiment seems to be the only tool for finding out if our conjecture is correct. One should keep in mind, however, that, even if a steady SSW exists for a certain set of parameters, this does not necessarily mean that it can be observed in an experiment, as it can be unstable with respect to three-dimensional disturbances (which we have not explored yet). In other words, a three-dimensional model of SSWs should be examined, similar to those considered for various asymptotic limits in Refs. [14–20]. It would also be interesting to examine how SSWs are affected by the liquid’s inertia (preliminary simulations with finite Reynolds number indicate that it is conducive to overturning).

Our results can also be extended to SSWs with $h^{(-)} = 0$, in which case the wave’s front is bounded by a contact line. One can conjecture that some of such SSWs still overturn (simply because overturning occurs near the “crest” of the wave and thus is not likely to be affected by what happens near the contact line). Then, if the liquid “splashes” onto the dry plate in front of the wave, the contact line will effectively “jump” forward. Then a new shock will form and break, causing another jump. Such dynamics are very different from the commonly used Tanner law and similar models.

Finally, note that the existence of a shock wave in an asymptotic model does not guarantee the existence of its Navier–Stokes counterpart (because the latter overturns). Such asymptotic solutions are meaningless physically (see examples discussed in Ref. [11]).

-
- [1] D. J. Benney, *J. Math. Phys.* **45**, 150 (1966).
 [2] C. C. Mei, *J. Math. Phys.* **45**, 266 (1966).
 [3] G. M. Homsy, *Lect. Appl. Math.* **15**, 191 (1974).
 [4] A. A. Nepomnyashchy, *Izv. Akad. Nauk SSSR, Mekh. Zhidk. Gaza* **3**, 28 (1974) [*Fluid Dyn.* **9**, 354 (1974)].
 [5] S. P. Lin, *J. Fluid Mech.* **63**, 417 (1974).
 [6] H.-C. Chang and E. A. Demekhin, *Complex Waves Dynamics on Thin Films* (Elsevier, Amsterdam, 2002).
 [7] A. Mavromoustaki, O. K. Matar, and R. V. Craster, *Phys. Fluids* **22**, 112102 (2010).
 [8] COMSOL Multiphysics 3.4, COMSOL Inc. [<http://www.comsol.com>].
 [9] O. Schenk and K. Gärtner, Pardiso solver project [<http://www.pardiso-project.org/>].
 [10] T. A. Davis, *ACM Trans. Mathematical Software* **30**, 196 (2003).
 [11] E. S. Benilov, V. N. Lapin, and S. B. G. O’Brien, *J. Eng. Math.* (submitted).
 [12] E. S. Benilov, S. J. Chapman, J. B. McLeod, J. R. Ockendon, and V. S. Zubkov, *J. Fluid Mech.* **663**, 53 (2010).
 [13] E. S. Benilov and O. A. Power, *Phys. Plasmas* **14**, 082101 (2007).
 [14] A. L. Bertozzi and M. P. Brenner, *Phys. Fluids* **9**, 530 (1997).
 [15] A. L. Bertozzi, A. Münch, X. Fanton, and A. M. Cazabat, *Phys. Rev. Lett.* **81**, 5169 (1998).
 [16] A. A. Nepomnyashchy, *Fluid Dynamics at Interfaces* (Cambridge University Press, Cambridge, 1999), pp. 85–98.
 [17] A. L. Bertozzi and M. Shearer, *SIAM J. Math. Anal.* **32**, 194 (2000).
 [18] A. L. Bertozzi, A. Münch, M. Shearer, and K. Zumbrun, *Euro. J. Appl. Math.* **12**, 253 (2001).
 [19] S. Kalliadasis, E. A. Demekhin, C. Ruyer-Quil, and M. G. Velarde, *J. Fluid Mech.* **492**, 303 (2003).
 [20] S. Saprykin, E. A. Demekhin, and S. Kalliadasis, *Phys. Fluids* **15**, 117105 (2005).